COLLISIONAL FORMATION OF SMOOTH-CRYSTALLINE MICROCHONDRULES IDENTIFIED IN UNEQUILIBRATED ORDINARY CHONDRITES. E. Dobrică and A. J. Brearley, Department of Earth and Planetary Sciences, MSC03-2040, 1University of New Mexico, Albuquerque, NM 87131-0001, USA (edobrica@unm.edu).

Introduction: Microchondrules are silicate, glassy spherules analogous to chondrules with sizes less than 40 μm [1]. They have been identified embedded within the fine-grained matrices and chondrule rims of unequilibrated ordinary chondrites (UOCs) [1-2]. Their shape and texture suggest that these objects have formed in the solar nebula by rapid cooling of melt droplets; however, the exact formation mechanism and their connection to chondrules remain unknown. In this study, a significant number of microchondrules were identified in the matrices and chondrule rims of the two UOCs (Semarkona - LL3.00 and MET 00526 - L3.05). The purpose of this study is to discuss the relationship between microchondrules and chondrules, to constrain the physico-chemical conditions of their formation and to understand the implications of their presence at the time when UOCs accreted.

Methods: Thin sections of MET 00526 and Semarkona were initially studied by Scanning Electron Microscopy (SEM) on a FEI Quanta 3D FEGSEM/FIB operating at 30 kV, using backscattered electron (BSE) imaging. After detailed SEM characterization, quantitative mineral analyses of microchondrules and chondrules were measured using a JEOL 8200 Superprobe electron microprobe (EMPA), operating at an accelerating voltage of 15 kV and a 20 nA beam current. Transmission Electron Microscopy (TEM) sections of microchondrules and chondrule rims (two from MET 00526 and one from Semarkona) were prepared using the focused ion beam (FIB) technique with a FEI Quanta 3D Dualbeam® FIB instrument. Bright and dark-field TEM images and quantitative EDS X-ray analyses were carried out at 200 kV on a JEOL 2010F FEG TEM/Scanning TEM (STEM).

Results: Microchondrules represent ~800 ppm of UOCs and are characterized either by porous-glassy, smooth-crystalline interiors or a melange of these two types [2]. SEM studies show that ~20-25% of type I (FeO-poor) chondrule rims from Semarkona and MET 00526 contain all these types of microchondrules (Figs. 1-3). One particular type IA chondrule from MET 00526 presents a rim of microchondrules which all have a similar dendritic texture (Fig. 2). The chemical compositions of microchondrules in this rim are similar to the chondrule silicate compositions (Fo_{97} – chondrule and Fo_{96} – microchondrule). Occasionally, we identified protuberances of silicate materials similar to those identified in the smooth-crystalline microchondrules (Fig. 1, 3) that extend from the chondrule periphery into the matrix. These protuberances are connected to the chondrules and terminate with a spherical shape (Fig. 1, 3).

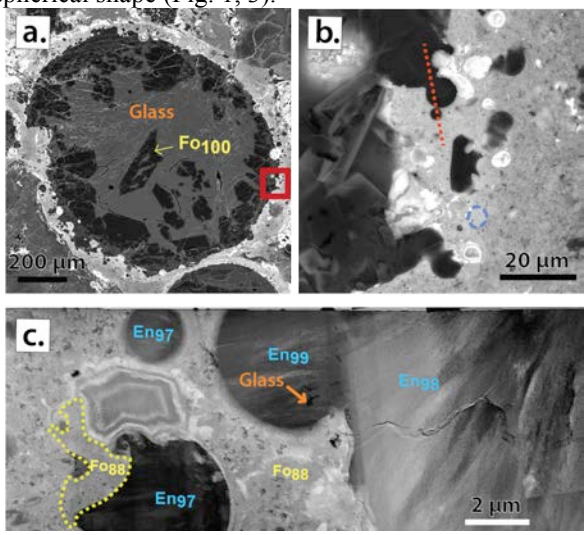

Figure 1. Backscattered electron SEM images (a-b) of a type IA PO (glass-rich) chondrule from MET 00526 showing the relationship between chondrule and microchondrules. a) The red box outlines the area shown in Fig. 1b. b) The red dashed line across the spherical protuberance and the smooth microchondrule shows the position of one FIB section prepared for TEM analysis (Fig. 1c). The blue dashed line shows the sharp boundary between the glassy microchondrule and the matrix. Dark-field STEM image (c) of the FIB section analyzed. The yellow dashed line shows the boundary between the porous material (Fo_{88}) and the matrix. En = low-Ca pyroxene, Fo = forsterite.

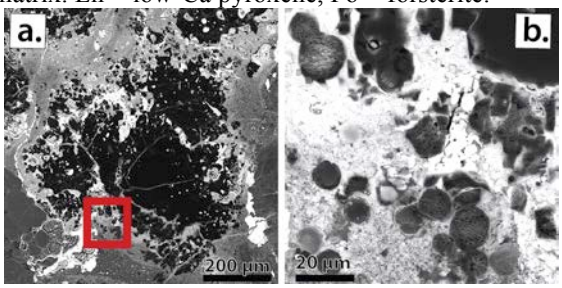

Figure 2. Backscattered electron SEM images of a type IA chondrule from MET 00526 showing the presence of a rim of microchondrules having the same chemical composition as the chondrule. The microchondrules in the rim of this chondrule all have the same dendritic texture. The red box outlines the area shown in Fig. 1b.

TEM studies show that these protuberances connected to chondrules are composed either of low-Ca pyroxene (En_{98-99}, Fig. 1) or olivine Fo_{83-100}, Al-rich glass (~77 wt% SiO_2 and ~19 wt% Al_2O_3, orange

dashed line in Fig. 3) containing glassy Na-rich inclusions (a few nm to 400 nm in size, the light-gray phase in the glass, 58 wt% SiO_2, 15 wt% Al_2O_3 and 25 wt% Na_2O, Fig. 3) and high-Ca pyroxene ($En_{56}Wo_{43}$). The microchondrules have similar chemical compositions and textures to the chondrules adjacent to them.

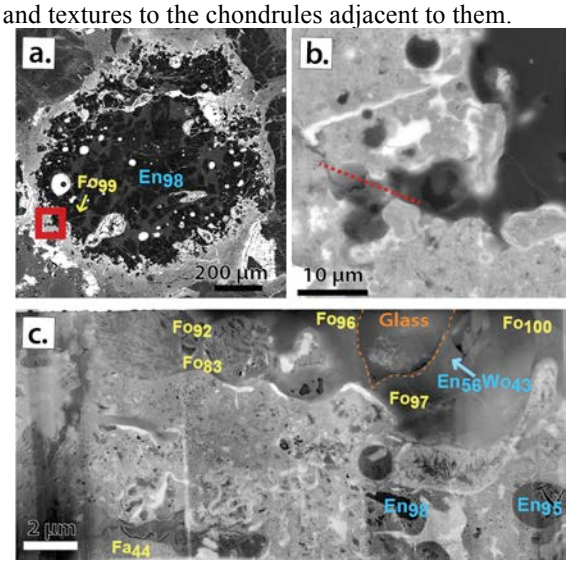

Figure 3. Backscattered electron SEM images (a-b) of a type IAB POP chondrule from MET 00526 showing the relationships between the chondrule and microchondrules. a) The red box outlines the area shown in Fig. 1b. b) The red dashed line across the protuberance shows the position of one FIB section prepared for TEM analysis (Fig. 1c). Dark-field STEM image (c) of the FIB sections (Fig. 1b) analyzed.

Discussion: Previous studies have shown that microchondrules may have been formed by remelting of the host chondrule surface and fine-grained FeO-rich dust [1, 3]. Our SEM and TEM observations provide new insights into the relationship between microchondrules and chondrules. We identified a considerable number of rims on type I chondrules from UOCs having texturally distinct, heterogeneously distributed, protuberances of silicate materials connected to the chondrules, ending with spherical, smooth-crystalline microchondrules. Their textures and chemical compositions suggest that these materials were pulled away or ejected from the surface of the chondrule during the time when the chondrules were molten. The occurrence of these distinct morphologies shows that the chondrules were disrupted, probably by collisions with other chondrules, when they were completely or partially melted. The preservation of protuberances and microchondrules suggest that the cooling rates were exceptionally fast. In addition, the skeletal and dendritic textures of several protruberances and microchondrules also suggest rapid cooling rates [4], much faster than the cooling rate necessary to form the porphyritic texture in the host chondrule. This effect is probably due to an increase in the surface area to volume ratio (SA:V) produced by the collisions that splatter or spall these small droplets of molten liquid. The increased SA:V ratio allowed more efficient removal of heat by radiation compared with the cooling rate of the larger parent chondrule. Based on surface tension calculations, the molten chondrules would be disrupted rather than fused if collisions took place at velocities greater than 130 cm s^{-1} and if the viscosity of the molten chondrule was greater than 1.2 x 10^5 Pa s [5-6]. Bischoff and Palme [7] suggested that the collision of two chondrules, while one of them was still partially molten, could easily lead to the splashing of melt droplets that would then form independent melt droplets. Other evidence of disruption during collisions is present in UOCs, such as microchondrules with more elongate, deformed shapes and a high frequency of compound microchondrules and chondrules (>5% of all chondrules) [6, 8].

The lack of microchondrules in the rims of type II (FeO-rich) chondrules from UOCs and in other types of chondrites suggest different liquidus temperatures, dynamic conditions and/or dust density compared to the type I chondrules from UOCs. The presence of microchondrule-rich clouds around only type I chondrules implies that the accretion of fine-grained dust rims onto some chondrules in UOCs occurred very rapidly after the microchondrules formed. However, a problem for the rapid accretion of these rims and, by implication, the parent-bodies of UOCs is the presence of microchondrules embedded in the fine-grained matrices of UOCs and the fact that chondrules within a single chondrite, formed over an extended period of more than a million years [e.g. 9].

Conclusion: Our observations show that the smooth-crystalline microchondrules and protuberances seem to have formed by materials splattered or spalled from the chondrules when they were still either completely or partially molten. The observational constrains presented by this study suggest that the cooling rates of the microchondrules and melt protuberances were different from the large chondrule.

Acknowledgements: This work was funded by NASA Cosmochemistry grants NNG06GG37G and NNX11AK51G to A. J. Brearley (PI).

References: [1] Krot A. N. et al. (1997) *Geochim. Cosmochim. Acta,* 61, 463-473. [2] Dobrică E. and Brearley A. J. (2013) LPSC XXXIV, Abstract #2701. [3] Krot A. N. and Rubin A. E. et al. (1996) *Chondrules and the protoplanetary disk*, pp. 181-186. [4] Hewins et al. (2005) *Chondrules and the protoplanetary disk*, pp. 286-316. [5] Kring D. A. (1991) *Earth and Planet. Sci. Letters,* 105, 65-80. [6] Ciesla F. J. et al. (2004) *Meteorit. Planet. Sci.* 39, 531-544. [7] Bischoff A. and Palme H. (1988) LPSC XIX, Abstract #86. [8] Wasson J. T. et al. (1995) *Geochim. Cosmochim. Acta,* 59, 1847-1869. [9] Jones R. H. (2012) *Meteorit. Planet. Sci.,* 47, 1176-1190.